

## Research Article

# Remediation of Chlorpyrifos-Contaminated Soils by Laboratory-Synthesized Zero-Valent Nano Iron Particles: Effect of pH and Aluminium Salts

A. Vijaya Bhaskar Reddy, V. Madhavi, K. Gangadhara Reddy, and G. Madhavi

Department of Chemistry, S.V. University, Tirupati 517502 A.P, India

Correspondence should be addressed to V. Madhavi; madhusvupg@gmail.com

Received 5 March 2012; Revised 19 July 2012; Accepted 23 July 2012

Academic Editor: Bruno Capaccioni

Copyright © 2013 A. Vijaya Bhaskar Reddy et al. This is an open access article distributed under the Creative Commons Attribution License, which permits unrestricted use, distribution, and reproduction in any medium, provided the original work is properly cited.

Degradation of the insecticide chlorpyrifos in contaminated soils was investigated using laboratory synthesized zero-valent nano iron (ZVNI) particles. The synthesized ZVNI particles were characterized as nanoscale sized by scanning electron microscopy (SEM) and transmission electron microscopy (TEM). The zero-valent state ( $\text{Fe}^0$ ) of iron was confirmed by EDAX analysis and the morphology of the ZVNI particles was studied by XRD. Batch experiments were conducted by treating the chlorpyrifos contaminated soil with ZVNI, our results indicate that 90% of chlorpyrifos was degraded after 10 days of incubation. Only 32% degradation was observed with micro zero-valent iron (mZVI) and no considerable degradation was attained without ZVNI. The degradation of chlorpyrifos followed the first-order kinetics with a rate constant and a half-life of  $0.245 \text{ day}^{-1}$  and 2.82 days, respectively. Degradation was monitored at two different pH values, that is, pH 10 and pH 4. Chlorpyrifos degradation rate constant increased as the pH decreases from 10 to 4. The corresponding rate constant and half-lives were  $0.43 \text{ day}^{-1}$  and 1.57 days for pH 4,  $0.18 \text{ day}^{-1}$  and 3.65 days for pH 10. In addition, an attempt was made by augmenting  $\text{Al}_2(\text{SO}_4)_3$  with ZVNI and it was found that the degradation rate of chlorpyrifos was greatly enhanced and the rate constant was rapidly increased from  $0.245 \text{ day}^{-1}$  to  $0.60 \text{ day}^{-1}$ . Hydrolysis and stepwise dechlorination pathway of chlorpyrifos with ZVNI was the dominant reaction.

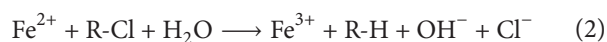
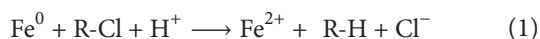
## 1. Introduction

Chlorpyrifos [O,O-diethyl O-3,5,6-trichloropyridin-2-yl phosphorothioate], an organophosphorous insecticide, is widely used worldwide in agriculture and residential pest control [1]. It is effective against a broad spectrum of insect pests on a variety of crops like grain, cotton, fruit, nut, and vegetable crops [2]. It has low water solubility,  $2 \text{ mgL}^{-1}$ , but it is highly soluble in many organic solvents [3]. Chlorpyrifos has high soil sorption coefficient ( $K_d = 13.4$  to  $1862 \text{ mL g}^{-1}$ ) depending on the soil type with a half-life of 10 to 120 days in different soils [4, 5]. Like other organophosphorous pesticides, its insecticidal action is due to the inhibition of the enzyme acetyl cholinesterase, resulting in the accumulation of the neurotransmitter, acetylcholine, at nerve endings [6, 7], this results in the excessive transmission of nerve impulses, which causes a potential risk to the humans and other organisms. Chlorpyrifos industry has developed fastly in

the past years worldwide, especially in some developing countries, such as China and India. Many disputes over chlorpyrifos were also happened in the aspect of application security for its high neurotoxicity. Recently, there are several reports indicating the presence of chlorpyrifos in cold drinks [8, 9], bottled drinking water and blood of farmers in Punjab, India. Therefore, more attention should be paid to the degradation of chlorpyrifos and their residues in the soil, water, and waste sites contaminated by chlorpyrifos. Conventionally, bioremediation is a good option for the degradation of chlorpyrifos, but it has several operational constraints, like slow rate of biodegradation, requiring long time, and incomplete degradation of chlorpyrifos gives more harmful degradation products [10]. Recently, nanotechnology represents a new generation of environmental technology that provides highly effective solutions to environmental cleanup and remediation by using zero-valent nano iron (ZVNI) (particle size 1–100 nm) as a chemical reductant [11].

The high effectiveness of ZVNI is due to its high surface area and surface reactivity, which is about 10–10,000 times higher than microscale zero-valent iron (mZVI) [12]. Pesticides which are persistent in aerobic environments are more readily degraded under reducing conditions [13], thus generating a reducing environment in contaminated soils. As a powerful reducing agent, zero-valent iron for reductive dechlorination of toxic halogenated pesticides attracted a great deal of attention since the 1980s [14].

Remediation with ZVNI can promote rapid abiotic degradation via reductive dehalogenation. When halogenated pesticide pollutants are treated with ZVNI, oxidation of ZVNI to Fe (II) provides electrons for dechlorination [15]. Under aerobic conditions, oxygen is the usual electron acceptor while, under anaerobic conditions,  $e^-$  release from the reaction of ZVNI with water can be coupled to the reaction of chlorinated compound according to the equations [16]:



ZVNI has been successfully used for remediation of halogenated pesticides and herbicides, chlorinated solvents, and heavy metal contaminants [17–19]. Based on relevant literature cited on pesticide treatment options, ZVNI-based remediation may be a feasible and attractive option. Iron is inexpensive, nontoxic and environmentally compatible. Researchers showed that ZVNI has been successfully used to transform halogenated pesticides, chlorinated solvents, and polychlorinated biphenyls [20].

The objective of the study described in this paper was to quantify the effectiveness of our laboratory synthesized zero-valent nano iron (ZVNI) to remediate chlorpyrifos contaminated soils and investigate the effect of pH and aluminium salts on the rate of degradation of chlorpyrifos. A pH stat was used to determine the change of pH during the degradation by ZVNI. Finally, the mechanism of the transformation of chlorpyrifos on treatment with ZVNI was analyzed according to the experimental results.

## 2. Materials and Methods

**2.1. Chemicals.** Chlorpyrifos (purity >99.9%) was purchased from Sigma-Aldrich (St. Louis, MO, USA). Commercial-grade Chlorpyrifos (Dursban 20EC) was obtained from Dow Agro Sciences, India. Fe (II) sulfate heptahydrate ( $\text{FeSO}_4 \cdot 7\text{H}_2\text{O}$ ), sodium borohydride ( $\text{NaBH}_4$ ), anhydrous sodium sulfate ( $\text{Na}_2\text{SO}_4$ ) and aluminium Sulfate [ $\text{Al}_2(\text{SO}_4)_3$ ] were procured in their highest grades available from Sigma-Aldrich (St. Louis, MO, USA). Ethanol, toluene, and all other solvents used were of analytical grade. Pure water was deionized and double distilled with a Milli-Q-water purification system (Millipore).

**2.2. Preparations of ZVNI Particles.** Unlike other conventional methods, ethanol was used as a stabilizer during the preparation of ZVNI particles. Preparation of ZVNI was achieved by the reduction of 30% ethanolic solution

of 1 M ferrous sulfate with equal volume of 1.6 M sodium borohydride ( $6 \text{ mL min}^{-1}$ ), addition of ethanol provides a protection layer for each iron nano particle. Here, the control of dropping rate is very important because quick addition may cause aggregation of ZVNI precipitates; in contrast very slow addition may cause the oxidation of nanoparticles which are formed sequentially. Ferrous iron was reduced and zerovalent iron particles were precipitated according to the equation [21]:



When all the nanoparticles were precipitated on the bottom of the beaker, the supernatant was removed, and then the solid iron nano particles were washed with ethanol. After thoroughly drying the nanoscale iron, air was allowed to slowly bleed over the iron for a period of approximately 8 h to passivate the iron. The resulting black clusters of iron were ground and fine ZVNI powder was stored under nitrogen environment for later use.

**2.3. Nanoparticle Characterization.** Transmission electron microscope (TEM) image was taken by using Philips TECHNAI FE 12 microscope. Morphological studies of the synthesized ZVNI particles were carried out by using scanning electron microscope (SEM) fitted with an Energy-Dispersive X-ray Analysis (EDAX) System (model CARL-ZEISS EVO MA 15). The sample was observed at 30,000 x magnification with an accelerating voltage of 20 kV. X-ray diffraction (XRD) analysis of ZVNI was performed using a Seifert 3003 TT X-ray diffractometer, the analysis was performed at 40 kV and 40 mA with  $\text{Cu-K}\alpha$  radiation at a wavelength of  $1.542 \text{ \AA}$ . Brunauer-Emmett-Teller (BET)-specific surface area of ZVNI was determined by  $\text{N}_2$  gas adsorption using Micromeritics ASAP-2000, USA. Microscale zero-valent iron particles (mZVI) were prepared by mechanically grinding the commercial fine iron powder to diminish the particle size by electrical mortar grinder with a 130-W motor.

**2.4. Extraction of Pesticide for GC-MS Analysis.** Chlorpyrifos was extracted from 20 g of soil in 50 mL Teflon centrifuge tubes by adding 30 mL toluene and agitated for a period of 4 h at 150 rpm on horizontal shaker at  $25^\circ\text{C}$ . The tubes were then centrifuged at  $4000 \times g$  for 10 min, and then the extract was filtered through anhydrous sodium sulfate and evaporated by using a rotary evaporator (Rotavapor R-210/R-215-BUCHI) at  $40^\circ\text{C}$ . To the filtrate, 1 mL of toluene was added and analyzed by GC-MS.

A GC-MS (JEOL GCMATE II GC-MS) was used for the detection of intermediate products of chlorpyrifos during the degradation. The GC was equipped with a HP-5MS capillary column ( $30 \text{ m} \times 0.025 \text{ mm i.d}$ ) in helium carrier gas ( $1 \text{ mL per min}$ ) and with splitless injection system. The column was initially maintained at  $90^\circ\text{C}$  for 5 min and then increased to  $290^\circ\text{C}$  at a rate of  $8^\circ\text{C per min}$  and hold at  $290^\circ\text{C}$  for 5 min. The injector and interface temperature were kept at  $280^\circ\text{C}$  and the source temperature at  $250^\circ\text{C}$ . The injection volume was  $1 \mu\text{L}$ . Mass spectra were obtained by the electron impact (EI) at 70 eV using SIM mode.

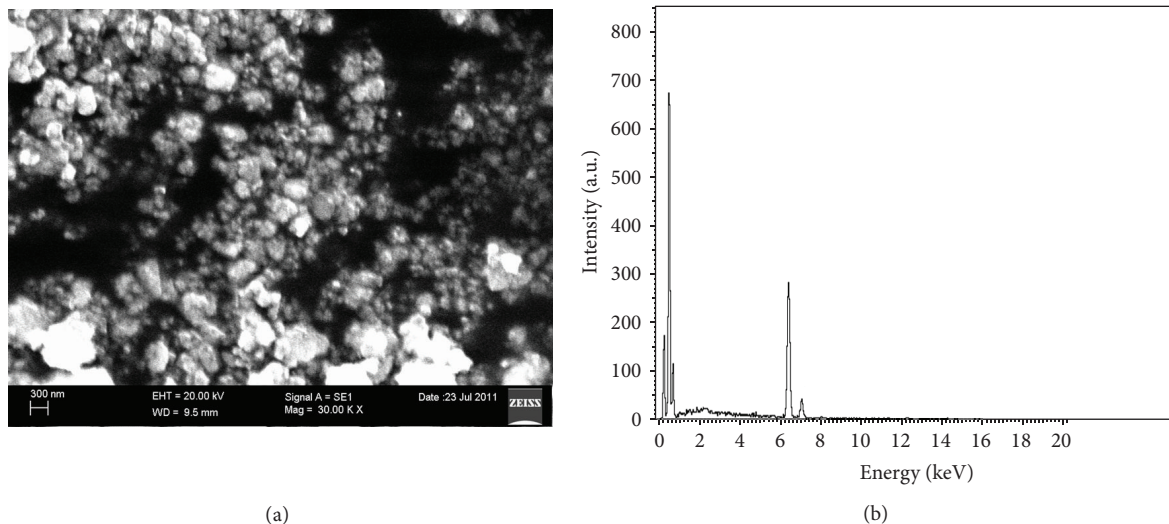


FIGURE 1: (a) SEM image of laboratory-synthesized ZVNI particles. (b) EDAX image of laboratory-synthesized ZVNI particles.

TABLE 1: Physicochemical properties of soil sample.

Soil properties	
pH	8.4
Texture	Red loamy soil
Organic matter (%)	0.857
Total nitrogen (%)	0.049
Cation exchange capacity (cmol kg <sup>-1</sup> )	4.3

**2.5. Soil Incubation Experiments.** Soil sample for the present study was collected from the field under cultivation without chlorpyrifos application previously, around Tirupati, Andhra Pradesh, India. Soil was air-dried and screened through a 2 mm sieve prior to hand milling. Standard soil nutrient, soil pH, soil texture, organic matter, and cation exchange capacity were determined in our laboratory. Different characteristics of soil sample are shown in Table 1. Soil was spiked with chlorpyrifos (dissolved in methanol) to get an initial concentration of 20 mg of chlorpyrifos per Kg of soil. Chlorpyrifos retained in soil was extracted with toluene as above. After that the aliquots were removed and transferred to 1.5 mL microcentrifuged tubes for GC-MS analysis. Results showed that the recovery of chlorpyrifos was always in the range between 95–98%.

20 g of chlorpyrifos contaminated soil was incubated in anaerobic condition with 0.2 g of ZVNI (1%) in 50 mL Teflon centrifuge tubes at 30°C and a soil/water content of 0.3 Kg/Kg. The sacrificial samplings were obtained after soil had been incubated for 2, 4, 6, 8, and 10 days, the trials were also conducted with micro-sized zero-valent iron (mZVI). The soil was extracted at preselected times with 30 mL toluene as described above and analyzed by GC-MS for identification of intermediates and HPLC for quantitative analysis.

An attempt was also made to carry out the influence of aluminium sulfate [Al<sub>2</sub>(SO<sub>4</sub>)<sub>3</sub>] on the destruction of

chlorpyrifos by ZVNI. 20 g of Chlorpyrifos-contaminated soil (20 mg Kg<sup>-1</sup>) was treated with 0.2 g (1%) of ZVNI and 0.2 g (1%) of [Al<sub>2</sub>(SO<sub>4</sub>)<sub>3</sub>], 6 mL 0.3 kg/kg(w/w) of water were added. The sacrificial samplings were obtained after soil had been incubated for 2, 4, 6, 8, and 10 days. The soil was extracted at preselected times with 30 mL toluene as described previously and analyzed by GC-MS.

### 3. Results and Discussion

**3.1. Characterizations of ZVNI Particles.** Scanning electron microscope (SEM) images of our laboratory-synthesized ZVNI particles show that the surface of ZVNI was rough and looked like aggregated round-shaped and the particle size distribution was in the range of 10–90 nm (Figure 1(a)). Transmission electron microscope (TEM) image shows that most of the particles size of ZVNI was less than 100 nm (Figure 2(a)). Compared to the previous results [21], the size of ZVNI particles of this study is even small and uniform. Ethanol was first introduced into ZVNI synthesis [22]; to prevent NZVI oxidation; however, we found that ethanol not only could prevent oxidation, but also acts as a stabilizer during ZVNI synthesis due to its organic properties. In addition, the surface area of ZVNI was significantly increased. XRD spectra of the synthesized ZVNI even show a little oxide peak, the very clear Fe<sup>0</sup> peak was also appeared (Figure 2(b)). As its support, XRD also indicated crystalline structure of the particles. Surface areas were determined by a Brunauer Emmett Teller (BET) N<sub>2</sub> gas adsorption desorption method at 77 K (Micromeritics ASAP-2000, USA). BET surface area analysis gave the surface area of ZVNI as 26.5 m<sup>2</sup> g<sup>-1</sup>. The average particle diameter was determined to be approximately 40 nm. The diameter is in accordance with that reported previously. According to the EDAX analysis of nanoscale Fe<sup>0</sup> particles, the composition was found as 86.72% of iron and 13.28% of oxygen (Figure 1(b)).

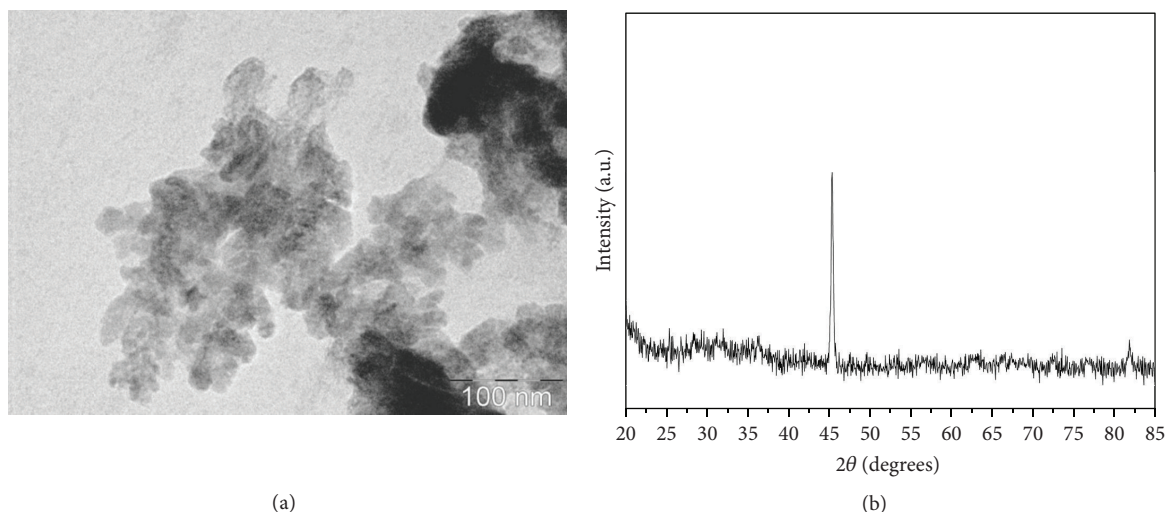


FIGURE 2: (a) Transmission electron microscope (TEM) image of laboratory-synthesized ZVNI. (b) XRD analysis of ZVNI particles.

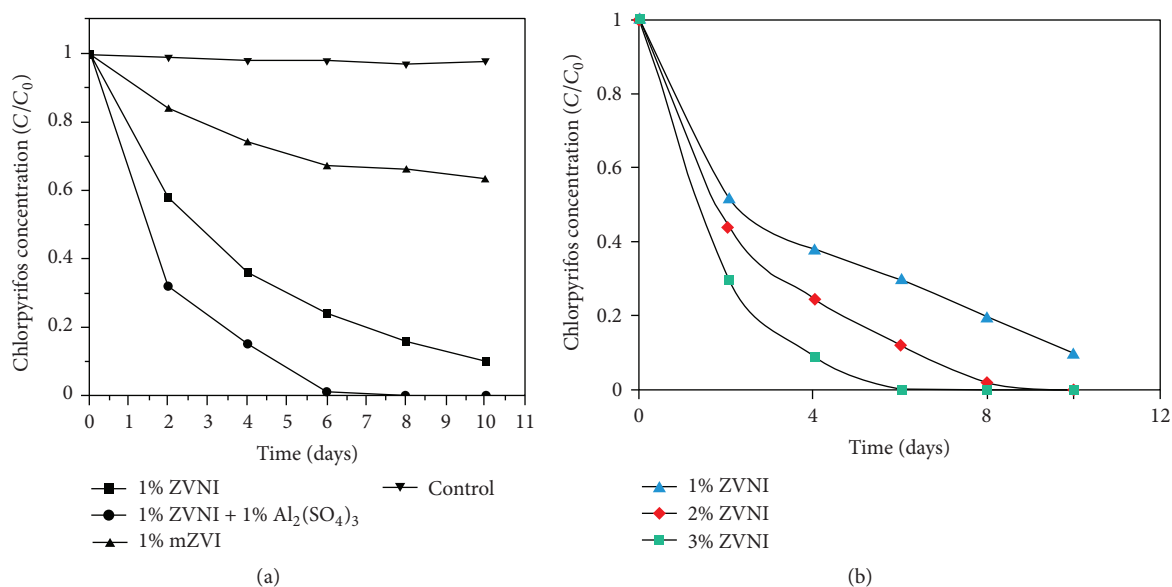
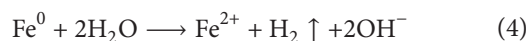


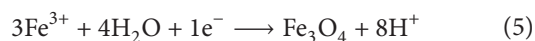
FIGURE 3: (a) Time-course degradation of chlorpyrifos with ZVNI. (b) Effect of ZVNI concentration on chlorpyrifos degradation.

**3.2. Degradation of Chlorpyrifos by ZVNI.** Rapid degradation of chlorpyrifos in all trials was observed, the initial chlorpyrifos concentration of  $20 \text{ mg L}^{-1}$  was decreased to 90% by reduction with ZVNI after 10 days of incubation. The relative persistence of commercial formulation of chlorpyrifos and its degradation rate were measured under anaerobic conditions in the laboratory. During the 10 days of incubation, the disappearance of chlorpyrifos was 90% with ZVNI, at the same time the disappearance of chlorpyrifos with mZVI was only 32% after 10 days of incubation (Figure 3(a)). The disappearance of chlorpyrifos with ZVNI followed the first-order kinetics (Figure 4). The calculated rate constant and half-life for the degradation of chlorpyrifos with ZVNI were  $0.245 \text{ day}^{-1}$  and 2.82 days respectively. We could be able to determine the feasibility of using 1% ZVNI (w/w) to remediate  $20 \text{ mg Kg}^{-1}$  chlorpyrifos contaminated soil. Soil

pH was increased due to reduction of  $\text{H}_2\text{O}$  by ZVNI in soil as per the equation:



Percentage of soil organic matter has not significantly changed during the 10 days incubation. Soil after treating with ZVNI showed the black compound and was found as magnetite by XRD analysis according to the equation:



ZVNI promotes dechlorination and hydroxylation of chlorinated compounds [18], chlorpyrifos degradation products were analyzed at preselected times during treatment. The GC-MS analysis showed that ZVNI is able to degrade Chlorpyrifos during the 10 days of incubation. Degradation efficiency

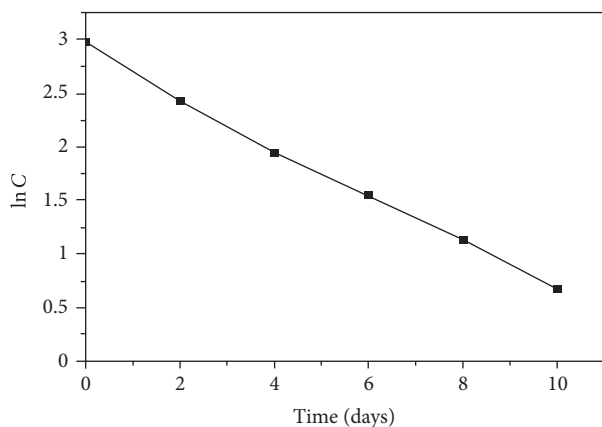


FIGURE 4: First-order kinetic model for chlorpyrifos degradation with ZVNI.

was increased with increasing the concentration of nano iron particles (Figure 3(b)), the degradation of chlorpyrifos was 90% after 10 days of incubation, and the quantitative analysis was done by comparing the peak area of standard chlorpyrifos. The major degradation product was TCP (3,5,6-trichloro-2-pyridinol). To analyze the degradation products of chlorpyrifos, the soil was extracted with toluene and analyzed by GC-MS. The results suggested that hydrolysis of chlorpyrifos were occurred followed by dechlorination using zero-valent nano iron, it was inferred that our laboratory-synthesized ZVNI is functioned well as a reductant to degrade chlorpyrifos structure.

**3.3. Effect of PH and Aluminium Sulfate on Chlorpyrifos Degradation.** Chlorpyrifos degradation by ZVNI was investigated under two pH conditions. We used a pH-stat apparatus (ELICO, LI-120) to control the pH in ZVNI-Chlorpyrifos matrix. To study the effect of soil pH on chlorpyrifos degradation, three replicates of different pH soils were treated with solution of chlorpyrifos dissolved in methanol to give a concentration of  $20 \text{ mg Kg}^{-1}$ . The soils were left on a laminar flow bench for 3 to 4 h to allow evaporation of the solvent, pH of the soil has been adjusted by adding  $\text{CaCO}_3$  (to increase soil pH to 10) and  $(\text{NH}_4)_2\text{SO}_4$  (to decrease soil pH to 4). Chlorpyrifos degradation rate constant was increased as the pH decreased from 10 to 4. Corresponding rate constant and half-lives were  $0.43 \text{ day}^{-1}$  and 1.57 day for pH 4, and they were  $0.18 \text{ day}^{-1}$  and 3.65 days for pH 10 (Figure 5). Slower destruction kinetics with increasing pH was previously observed with metachlor treatment [18]. The reason of this is the formation of secondary reductants Fe(II) or Fe(II)-containing oxides and hydroxides on the surface of ZVNI, which hinders the degradation. Lower pH would remove these passivating layers from ZVNI core and makes it free for further reaction with halogenated pesticides. Moreover, acid hydrolysis facilitates the degradation of chlorpyrifos at lower pH. Hence this process is strongly pH-dependent, since hydrolysis of chlorpyrifos was observed effectively at lower pH.

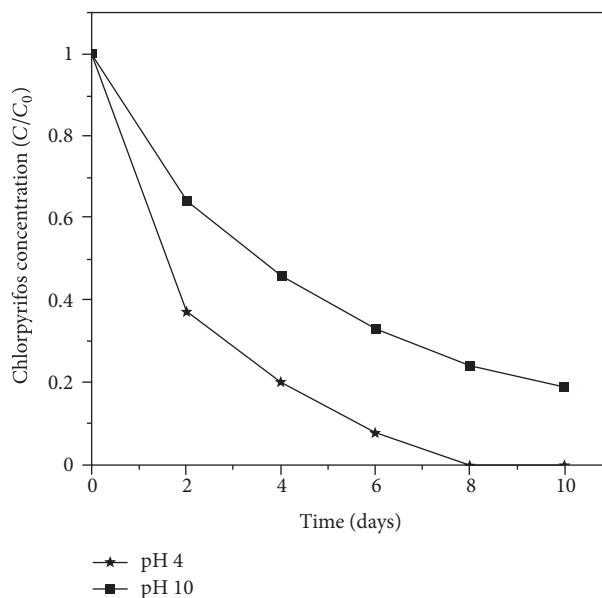


FIGURE 5: Time-course degradation of chlorpyrifos at different pH values.

Chlorpyrifos degradation efficiency was enhanced when  $[\text{Al}_2(\text{SO}_4)_3]$  was added to the soil. In soil incubation experiment, ZVNI with aluminium sulfate salt had successfully removed the total chlorpyrifos after 6 days of incubation. The rate constant was rapidly increased from  $0.24 \text{ day}^{-1}$  to  $0.60 \text{ day}^{-1}$ , this indicates that rapid degradation of chlorpyrifos was noticed when ZVNI was augmented with  $\text{Al}_2(\text{SO}_4)_3$  because high concentration of aluminium salts can restrict passivation by moving the reaction products away from ZVNI surface [23]. This supports that availability of Al(III), Fe(II) and Fe(III) during ZVNI oxidation results in increasing Fe(II) in the chlorpyrifos treatment system and thus favoring its degradation. Small, high-charge exchangeable cations, such as Al(III) or Fe(III), produce Bronsted acidity by promoting a reaction with water to release  $\text{H}^+$  ions. The ranking potential Bronsted acid strength for Al(III) is high [24]; hence, Al can act as a Lewis acid by coordinating the moieties of some organic contaminants, bringing them closer to the surface of ironoxides for reductive transformation.

**3.4. Degradation Pathway.** During the initial reaction period of chlorpyrifos, TCP was the most predominant by product. The reductive dechlorination by successive loss of chloride ions was confirmed as the main pathway of degradation of chlorpyrifos with ZVNI. It is in agreement with several studies of dechlorinated compounds [25]. According to the by product analysis, the base peak at  $m/z$  197 was identified as the major degraded product TCP. The main fragment ion spectrum of the peak at  $m/z$  197,  $m/z$  131,  $m/z$  97,  $m/z$  111,  $m/z$  95,  $m/z$  127, and  $m/z$  115 are the major dechlorination products of TCP. The peak at  $m/z$  169 was due to the formation of (DETP) 0,0-diethyl thiophosphate which was formed on the hydrolysis of chlorpyrifos (Table 2). The fragment ion peak at  $m/z$  141 was due to the loss of  $\text{C}_2\text{H}_5\text{OH}$

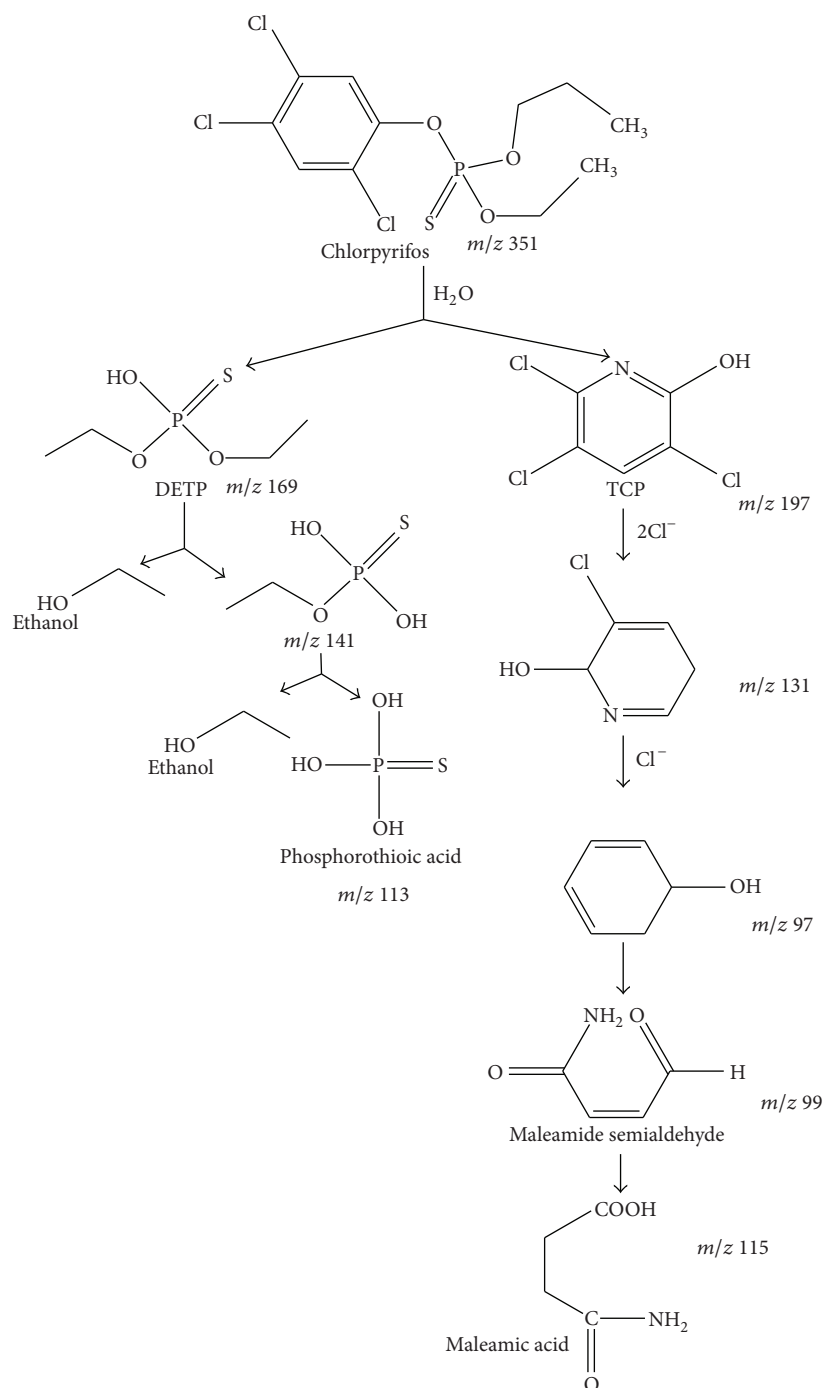


FIGURE 6: Proposed pathway for the degradation of chlorpyrifos by ZVNI particles.

from DETP, and the peak at  $m/z$  113 was due to the formation of phosphorothioic acid. In addition to above, the peak at  $m/z$  314 corresponds to  $[M-HCl]^+$  and the peaks at 286, 258 correspond to the removal of one and two ethylene molecules from  $[M-HCl]^+$ . The first step in the reductive transformation is the formation of TCP. TCP's continuous dechlorination resulted in the formation of maleamic acid and another byproduct DETP was transformed to phosphorothioic acid. Hence, the degradation of chlorpyrifos with ZVNI had occurred through a stepwise dechlorination mechanism.

The proposed intermediates and pathway with the sequential reductive dechlorination of chlorpyrifos by ZVNI are shown (Figure 6) according to the byproduct analysis.

#### 4. Conclusion

The results of the present investigation showed that ZVNI can be successfully used to remediate the soils contaminated with chlorpyrifos under anoxic environment at ambient temperature and pressure. Hydrolysis followed by reductive

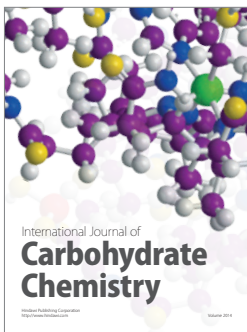
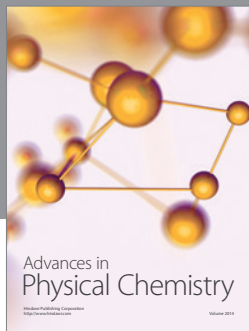
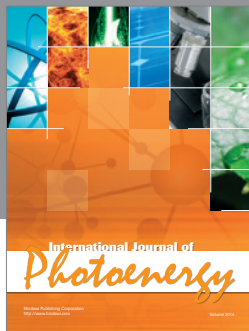
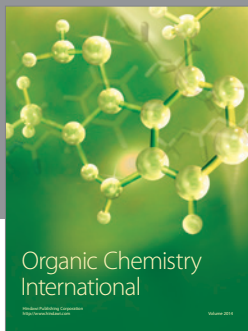
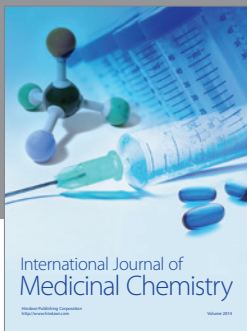
TABLE 2: Major fragmentation peaks of chlorpyrifos with  $m/z$  values.

Fragmentation peaks	$m/z$ values
TCP	197, 198, 199, 200 (indicates 3 Cl atoms)
DETP	169
Phosphorothioic acid	113
Maleamic acid	115

dechlorination was the major process in degradation of chlorpyrifos by ZVNI. The dechlorination product was maleamic acid. The dechlorinated product is environmentally benign and more biodegradable than its parent compound chlorpyrifos. Lowering the pH from 10 to 4 increases the destruction kinetic rates of chlorpyrifos by ZVNI. From the results, it can be suggested that ZVNI may be applicable for the remediation of concentrated chlorpyrifos contaminated soils. Moreover, aluminium salts can successfully increase the destruction of chlorpyrifos by ZVNI, the degradation of chlorpyrifos mainly seemed to be a stepwise dechlorination process. This is for the first time that chlorpyrifos has been degraded under reductive environment using ZVNI. Results from this study can be applied for on-site treatment of soil with high concentrations of chlorpyrifos contamination.

## References

- [1] C. M. H. Cho, A. Mulchandani, and W. Chen, "Bacterial cell surface display of organophosphorus hydrolase for selective screening of improved hydrolysis of organophosphate nerve agents," *Applied and Environmental Microbiology*, vol. 68, no. 4, pp. 2026–2030, 2002.
- [2] W. J. Hayes and E. R. Laws, *Classes of Pesticides*, vol. 3, Academic Press, New York, NY, USA, 1990.
- [3] K. D. Racke, D. A. Laskowski, and M. R. Schultz, "Resistance of chlorpyrifos to enhanced biodegradation in soil," *Journal of Agricultural and Food Chemistry*, vol. 38, no. 6, pp. 1430–1436, 1990.
- [4] M. T. Moore, R. Schulz, C. M. Cooper, S. Smith, and J. H. Rodgers, "Mitigation of chlorpyrifos runoff using constructed wetlands," *Chemosphere*, vol. 46, no. 6, pp. 827–835, 2002.
- [5] S. Pandey and D. K. Singh, "Total bacterial and fungal population after chlorpyrifos and quinalphos treatments in groundnut (*Arachis hypogaea* L.) soil," *Chemosphere*, vol. 55, no. 2, pp. 197–205, 2004.
- [6] P. K. Pradnya, B. J. Bhadbhade, N. M. Deshapande, and S. S. Sarnaik, *Indian National Science Academy*, vol. 70, no. 1, pp. 57–70, 2004.
- [7] L. A. Ee, H. Zhao, and J. P. Obbard, "Recent advances in the bioremediation of persistent organic pollutants via biomolecular engineering," *Enzyme and Microbial Technology*, vol. 37, no. 5, pp. 487–496, 2005.
- [8] Centre for Science and environment, How safe is bottled water? The Hindu, 2003.
- [9] Centre for science and environment, Pesticide cocktail poisons Punjab Villagers. The Hindu, 2005.
- [10] M. Bavcon Kralj, M. Franko, and P. Trebše, "Photodegradation of organophosphorus insecticides—investigations of products and their toxicity using gas chromatography-mass spectrometry and AChE-thermal lens spectrometric bioassay," *Chemosphere*, vol. 67, no. 1, pp. 99–107, 2007.
- [11] C. B. Wang and W. X. Zhang, "Synthesizing nanoscale iron particles for rapid and complete dechlorination of TCE and PCBs," *Environmental Science and Technology*, vol. 31, no. 7, pp. 2154–2156, 1997.
- [12] W. X. Zhang, "Nanoscale iron particles for environmental remediation: an overview," *Journal of Nanoparticle Research*, vol. 5, no. 3-4, pp. 323–332, 2003.
- [13] S. D. Comfort, P. J. Shea, T. A. Machacek, H. Gaber, and B. T. Oh, "Field-scale remediation of a metolachlor-contaminated spill site using zerovalent iron," *Journal of Environmental Quality*, vol. 30, no. 5, pp. 1636–1643, 2001.
- [14] T. Dombek, E. Dolan, J. Schultz, and D. Klarup, "Rapid reductive dechlorination of atrazine by zero-valent iron under acidic conditions," *Environmental Pollution*, vol. 111, no. 1, pp. 21–27, 2001.
- [15] R. A. Doong and Y. L. Lai, "Effect of metal ions and humic acid on the dechlorination of tetrachloroethylene by zerovalent iron," *Chemosphere*, vol. 64, no. 3, pp. 371–378, 2006.
- [16] D. R. Burris, T. J. Campbell, and V. S. Manoranjan, "Sorption of trichloroethylene and tetrachloroethylene in a batch reactive metallic iron-water system," *Environmental Science and Technology*, vol. 29, no. 11, pp. 2850–2855, 1995.
- [17] G. D. Sayles, G. You, M. Wang, and M. J. Kupferle, "DDT, DDD, and DDE dechlorination by zero-valent iron," *Environmental Science and Technology*, vol. 31, no. 12, pp. 3448–3454, 1997.
- [18] T. Satapanajaru, S. D. Comfort, and P. J. Shea, "Enhancing metolachlor destruction rates with aluminum and iron salts during zerovalent iron treatment," *Journal of Environmental Quality*, vol. 32, no. 5, pp. 1726–1734, 2003.
- [19] D. W. Blowes, C. J. Ptacek, and J. L. Jambor, "In-situ remediation of Cr(VI)-contaminated groundwater using permeable reactive walls: laboratory studies," *Environmental Science and Technology*, vol. 31, no. 12, pp. 3348–3357, 1997.
- [20] S. H. Joo and D. Zhao, "Destruction of lindane and atrazine using stabilized iron nanoparticles under aerobic and anaerobic conditions: effects of catalyst and stabilizer," *Chemosphere*, vol. 70, no. 3, pp. 418–425, 2008.
- [21] H. L. Lien and W. X. Zhang, "Nanoscale iron particles for complete reduction of chlorinated ethenes," *Colloids and Surfaces A*, vol. 191, no. 1-2, pp. 97–105, 2001.
- [22] S. M. Ponder, J. G. Darab, and T. E. Mallouk, "Remediation of Cr(VI) and Pb(II) aqueous solutions using supported, nanoscale zero-valent iron," *Environmental Science and Technology*, vol. 34, no. 12, pp. 2564–2569, 2000.
- [23] J. Farrell, M. Kason, N. Melitas, and T. Li, "Investigation of the long-term performance of zero-valent iron for reductive dechlorination of trichloroethylene," *Environmental Science and Technology*, vol. 34, no. 3, pp. 514–521, 2000.
- [24] M. C. McBride, *Environmental Chemistry of Soils*, Oxford University Press, New York, NY, USA, 1994.
- [25] F. W. Chuang, R. A. Larson, and M. S. Wessman, "Zero-valent iron-promoted dechlorination of polychlorinated biphenyls," *Environmental Science & Technology*, vol. 29, no. 9, pp. 2460–2463, 1995.



**Hindawi**

Submit your manuscripts at  
<http://www.hindawi.com>

